A Single-Phase Rectifier Having Two Independent Voltage Outputs With Reduced Fundamental Frequency Voltage Ripples

Wen-Long Ming and Qing-Chang Zhong, *Senior Member, IEEE*

***Abstract*—Half-bridge rectifiers are able to provide two voltage outputs, which offers three voltage levels, but the two voltage outputs depend on each other and also on system parameters. Moreover, the two voltage outputs contain large ripples because the currents following through the split capacitors contain significant fundamental-frequency components. In this paper, after analyzing the drawbacks of half-bridge rectifiers in detail, an independently controlled neutral leg is added to conventional half-bridge rectifiers to address these drawbacks. Furthermore, the associated decoupling control strategies are proposed. The rectification leg from the conventional half-bridge rectifier is controlled to maintain the dc-bus voltage and to draw a clean sinusoidal current that is in phase with the supply voltage. The neutral leg is controlled with a PI-repetitive controller to regulate one voltage output and also to provide the current path for any dc and/or fundamental-frequency components. As a result, the two voltage outputs are regulated independently and are robust against system parameters. The output voltage ripples are also reduced, and hence, the required capacitance to achieve the same level of voltage ripples is reduced. Experimental results are provided to validate the performance of the proposed single-phase rectifiers having two independent voltage outputs.**

***Index Terms*—Half-bridge, independent voltage outputs, single-phase rectifier, voltage ripples.**

I. Introduction

DUE to the penetration of renewable energy systems, more and more microgrids are connected to the public power grid via power converters [1]. In both ac and dc microgrids, ac is always rectified to dc when supplying dc loads and ac/ac conversion often needs dc as an intermediate step. In many circumstances [1]–[4], it is quite normal to have single-phase utilities so single-phase rectifiers are very popular [5]–[9]. A typical application of rectifiers is shown in Fig. 1, where it is often needed to provide two separate voltage outputs with the presence of a neutral line so that it is possible to power loads at three different voltage levels [10]. For example, many electronic systems need ± 5 V and/or ± 15 V. Rectifiers based on conventional half-bridge rectifiers, as shown in Fig. 2, are very attractive because they can provide two voltage outputs at relatively low costs.

However, the performance of the half-bridge rectifier could be reduced because of two main drawbacks. First, the two outputs are dependent on each other and also on the system parameters such as loads, capacitors and the source voltage [7], [11]. Because of this, it is hard to obtain two independent voltage outputs, which are expected to be the same or different from each other, according to the requirements of the loads. Moreover, the regulation range of the two outputs is limited by the ratio of the dual loads (R_+ and R_-). To be more precise, when operating with dual loads, the output voltages completely depend on the ratio of the dual loads. What is even worse is that, when operating with only one of the dual loads, the half-bridge rectifier cannot work properly. This is because dc capacitors are incapable of providing any dc currents. Moreover, as the source current is provided by charging and discharging the dc capacitors, the resulting large voltage ripples can be another serious problem and bulky electrolytic capacitors are often needed to level and smooth the ripples. However, for volume-critical and/or weight-critical systems like electrical vehicles and aircraft power systems, it is preferred to reduce the required bulky capacitors to enhance the power density. For systems with batteries and fuel cells, large ripple currents and ripple voltages could considerably reduce the lifetime of batteries and fuel cells too [12]–[14].

For the first drawback, there is very few research contributing to obtaining independent voltage outputs. Most of the previous research was focused on balancing the two voltages. Two main approaches have been reported in the literature. One of them is done at the ac side either through injecting a dc component into the ac input current [7] or through adding switches in parallel with the ac source [8]. However, according to the IEEE 1547 standard, the maximum permitted dc bias in the grid current is 0.5% of the rated value. Many other strategies can be found in [15], most of which also focus on strategies at the ac side. Although the voltage imbalance can be eliminated to some extent, these strategies suffer from low input power factor and/or limited voltage regulation range determined by the ratio of the dual loads. Another approach is done at the dc side through adding balancing circuits, which are put across the dc bus, and then, connected to the midpoint of the capacitors. In [10], a bidirectional buck/boost converter composed of two switches and two inductors was used for this purpose. Due to its topological

Manuscript received May 19, 2014; revised July 22, 2014; accepted August 1, 2014. Date of publication August 18, 2014; date of current version February 13, 2015. A preliminary version of this paper was presented at IEEE Energy Conversion Congress and Exposition, Denver, CO, USA, September 2013. Recommended for publication by Associate Editor R. Redl.

W.-L. Ming is with the Department of Automatic Control and Systems Engineering, The University of Sheffield, Sheffield S1 3JD, U.K. (e-mail: wenlongming@gmail.com).

Q.-C. Zhong is with the Department of Automatic Control and Systems Engineering, The University of Sheffield, Sheffield S1 3JD, U.K., and also with the China Electric Power Research Institute, Beijing 100192, China (e-mail: zhongqc@ieee.org).

Color versions of one or more of the figures in this paper are available online at http://ieeexplore.ieee.org.

Digital Object Identifier 10.1109/TPEL.2014.2348871

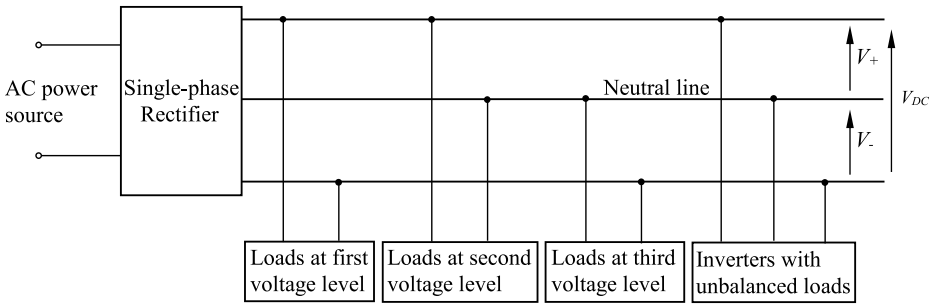

Fig. 1. Typical application of half-bridge rectifiers.

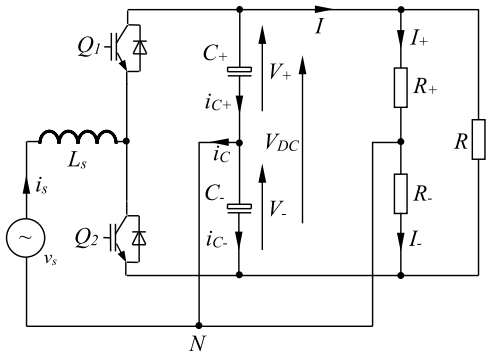

Fig. 2. Conventional single-phase half-bridge rectifier.

structure, this strategy also benefits with the resolved shoot-through problem. The circuit studied in [16]–[19] is shown to have the capability of balancing two voltages and creating a neutral line but it has not been applied to half-bridge rectifiers.

For the second drawback, it is worth noting that the voltage ripples in a half-bridge rectifier consists of a fundamental component and a second-order component [11]. The fundamental one is due to the topological structure, which is an unique feature for half-bridge rectifiers. On the other hand, the second order one is caused by the pulsating input power, which is a common feature for all single-phase rectifiers. The mixture of these two components makes the output voltage ripples of conventional half-bridge rectifiers much larger than that of conventional full-bridge rectifiers. How to reduce the second-order component of voltage ripples has been extensively studied for different single-phase rectifiers [9], [20], [21]. However, to the best knowledge of the authors, how to eliminate the fundamental component of ripples in half-bridge rectifiers has not been reported in the literature.

In this paper, the main drawbacks of conventional half-bridge rectifiers are analyzed in details at first. After that, the neutral leg used in [16]–[19] and [22] is put across the dc bus, linking to the midpoint of the split capacitors of conventional half-bridge rectifiers, to form a new topology for single-phase rectifiers. With the help of the neutral leg, the two voltage outputs become independent from each other and robust against parameter variations in loads and capacitors. Note that the two voltages can be different or the same, which only depend on the load requirements. What is important is that the difference of the two voltages does not cause any problem to the input current regulation [11] because of the decoupled control strategies adopted. This means the total harmonic distortion (THD) of the input current and the input power factor are not affected by the voltage difference either. The unity power factor can always be achieved as well because the input current can be easily controlled to be in phase with the input voltage. Moreover, in order to obtain two independent bidirectional dc output voltages, more than six active switches are often needed but the proposed topology only needs four active switches, which reduces the cost. This is probably the topology with the minimum number of active switches to form a bi-directional converter with two independent voltage outputs that could supply three loads at the same time. Another benefit of the topology is that the output voltage ripples can be reduced because the fundamental current component that originally flows through the split capacitors can be diverted and flows through the neutral leg. As a result, the required capacitors become smaller in order to achieve the same level of voltage ripples. Together with the rectification leg from a conventional half-bridge rectifier, the formed rectifier consists of two legs. The control of these two legs are independent, which makes the design of control strategies very flexible. In this paper, a repetitive controller is designed to regulate the current drawn from the grid so that the dc-bus voltage is maintained and a parallel PI-Repetitive controller is designed for the neutral leg to achieve excellent voltage regulation capability even with different loads and/or different capacitors.

The rest of this paper is organized as follows. The drawbacks of conventional half-bridge rectifiers are analyzed in detail in Section II. In Section III, the topology of the proposed single-phase rectifier is given. After that, operation principles of the rectifier with a neutral leg are discussed in detail. The associated control strategies are developed in Section IV, with experimental results presented in Section V. The proposed topology is then compared with a two-stage rectifier that consists of a power factor correction (PFC) converter and two dual-active-bridge (DAB) converters in Section VI. Conclusions are made in Section VII.

II. Drawbacks of Conventional Half-bridge Rectifiers

A. Average Circuit Model and Ripple Analysis

Assume that V_+ and V_- are the voltages across the capacitors C_+ and C_-, respectively. Then, the dc-bus voltage is

$$V_{\rm DC} = V_+ + V_-. \tag{1}$$

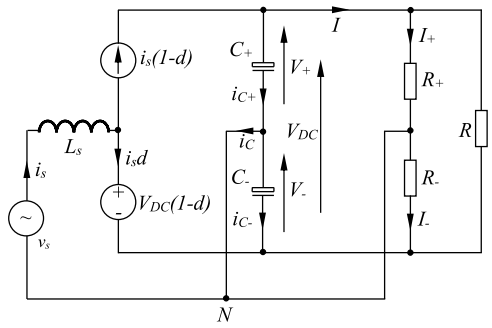

Fig. 3. Average circuit model of the conventional half-bridge rectifier.

Also, assume the source current of the rectifier is regulated to be sinusoidal as

$$i_s = I_s \sin \omega t \tag{2}$$

and in phase with the source voltage

$$v_s = V_s \sin \omega t \tag{3}$$

where V_s and I_s are the peak values of the input voltage and current, respectively, and ω is the angular line frequency. In this case, the power factor is unity, which is preferred in many applications. The average circuit model can be built as shown in Fig. 3, according to [11]. The switches Q_1 and Q_2 are replaced with a current source $i_s(1-d)$ and a voltage source $V_{\rm DC}(1-d)$, respectively, where d is the duty cycle of Q_2. To the best knowledge of the authors, all the analysis in the literature are based on the assumption that the split capacitors are the same and/or the dual loads are the same [7], [8], [11]. However, this assumption is hard to meet because the capacitors can easily become different due to their inevitable degradation. Since the loads may be different too, it is desirable that the two voltage outputs can be independent even when different loads are connected [10]. For this reason, detailed analysis about half-bridge rectifiers with different split capacitors and different loads is carried out in the sequel.

In order to obtain the unity power factor, the two switches are operated complementarily to track the reference source current, which is in phase with the source voltage. As the switching frequency is much higher than the line frequency, the duty cycle of switch Q_2 can be given by

$$d = \frac{V_+}{V_{\rm DC}} - \frac{V_s}{V_{\rm DC}} \sin \omega t \tag{4}$$

as demonstrated in [8] and [11]. According to the average circuit model shown in Fig. 3, the capacitor currents can be calculated as

$$i_{C+} = i_s(1-d) - \left(\frac{V_+}{R_+} + \frac{V_{\rm DC}}{R}\right) \tag{5}$$

$$i_{C-} = -i_s d - \left(\frac{V_-}{R_-} + \frac{V_{\rm DC}}{R}\right). \tag{6}$$

After substituting (2) and (4) into (5), there is

$$i_{C+} = \frac{V_- I_s}{V_{\rm DC}} \sin \omega t - \frac{V_s I_s}{2V_{\rm DC}} \cos 2\omega t + \frac{V_s I_s}{2V_{\rm DC}} - \left(\frac{V_+}{R_+} + \frac{V_{\rm DC}}{R}\right). \tag{7}$$

This can be rewritten as

$$i_{C+} = \frac{V_- I_s}{V_{\rm DC}} \sin \omega t - \frac{V_s I_s}{2V_{\rm DC}} \cos 2\omega t + \frac{V_-}{V_{\rm DC}} \left(\frac{V_-}{R_-} - \frac{V_+}{R_+}\right) \tag{8}$$

after taking into account the following power balance between the ac side and the dc side when ignoring the losses

$$\frac{V_s I_s}{2} = \frac{V_+^2}{R_+} + \frac{V_-^2}{R_-} + \frac{V_{\rm DC}^2}{R}. \tag{9}$$

Similarly, i_{C-} can be obtained as

$$i_{C-} = -\frac{V_+ I_s}{V_{\rm DC}} \sin \omega t - \frac{V_s I_s}{2V_{\rm DC}} \cos 2\omega t + \frac{V_+}{V_{\rm DC}} \left(\frac{V_+}{R_+} - \frac{V_-}{R_-}\right). \tag{10}$$

It is clear that there are a fundamental-frequency component, a second-harmonic component, and a dc component in both currents. Because these are currents flowing through capacitors, the dc components have to be zero; see the next section for more details. The second-harmonic component is a common feature existing in all single-phase rectifiers, which is caused by the pulsating input power [5], [9], [21]. However, the fundamental component is unique for half-bridge rectifiers. After integrating the current i_{C+} and i_{C-}, it can be obviously seen that the peak–peak fundamental-frequency voltage ripples over C_+ and C_- are $\frac{V_- I_s}{\omega C_+ V_{\rm DC}}$ and $\frac{V_+ I_s}{\omega C_- V_{\rm DC}}$, respectively, which are at least four times of the second-harmonic ripples because $\frac{V_- I_s}{\omega C_+ V_{\rm DC}} > 4\frac{V_s I_s}{4\omega C_+ V_{\rm DC}}$ and $\frac{V_+ I_s}{\omega C_- V_{\rm DC}} > 4\frac{V_s I_s}{4\omega C_- V_{\rm DC}}$. The voltage ripples can be very large if C_+ and C_- are small, and hence, it is important and desirable to make sure that no fundamental component exists in the current. The ripple ratio of the fundamental component is $\frac{V_- C_-}{V_+ C_+}$ and the ripple ratio of the second-harmonic component is $\frac{C_-}{C_+}$.

B. Operational Limit Caused by Loads

According to (8) and (10), there is a dc component in both currents. However, it is well known that no dc current can flow through capacitors, and thus, the dc components $\frac{V_-}{V_{\rm DC}}\left(\frac{V_-}{R_-} - \frac{V_+}{R_+}\right)$ and $\frac{V_+}{V_{\rm DC}}\left(\frac{V_+}{R_+} - \frac{V_-}{R_-}\right)$ must be equal to 0, which means the following condition:

$$\frac{V_+}{R_+} = \frac{V_-}{R_-} \tag{11}$$

must be satisfied. Hence, the voltages of the capacitors must be in proportion to the ratio of the dual loads, i.e., $\frac{V_+}{V_-} = \frac{R_+}{R_-}$, in the same way as a voltage divider. Since $V_+ + V_- = V_{\rm DC}$, the

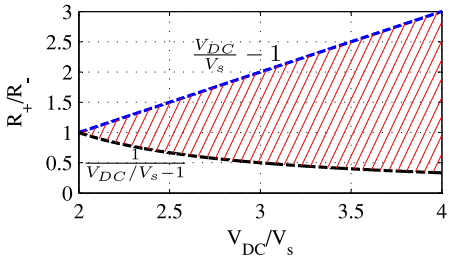

Fig. 4. Operation limit determined by the load ratio $\frac{R_+}{R_-}$ and the voltage boost factor $\frac{V_{\rm DC}}{V_s}$.

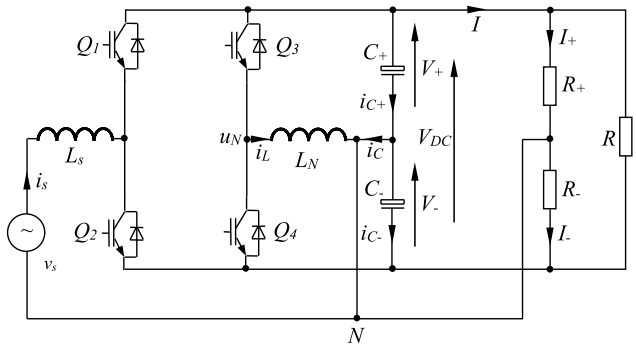

Fig. 5. Proposed single-phase rectifier with a neutral leg.

voltages can be found as

$$V_+ = \frac{V_{\rm DC}\frac{R_+}{R_-}}{1+\frac{R_+}{R_-}}$$

$$V_- = \frac{V_{\rm DC}}{1+\frac{R_+}{R_-}}.$$

Also, V_+ and V_- should be larger than V_s in order to ensure the normal operation of the rectifier. As a result, the load ratio $\frac{R_+}{R_-}$ needs to satisfy the following condition:

$$\frac{1}{\frac{V_{\rm DC}}{V_s}-1} < \frac{R_+}{R_-} < \frac{V_{\rm DC}}{V_s}-1 \tag{12}$$

where $\frac{V_{\rm DC}}{V_s}$ is the voltage boost ratio. This characterizes the operational limit of the rectifier, as shown in Fig. 4. For a given voltage boost ratio, the load ratio can only be chosen within the sector shaded by the red lines. This may considerably limit the application of half-bridge rectifiers.

If only a single load R is connected, then $R_+ = R_- = +\infty$. The condition (11) can be naturally satisfied because $\frac{V_+}{R_+} = \frac{V_-}{R_-} \equiv 0$. In this case, the rectifier can be operated for any load R.

If only one of the dual loads R_+ and R_- is connected, then one of $\frac{V_+}{R_+}$ and $\frac{V_-}{R_-}$ is equal to 0 but the other one is not. As a result, the condition $\frac{V_+}{R_+} = \frac{V_-}{R_-}$ cannot be satisfied. This means that the conventional half-bridge rectifier cannot work with only one of the dual loads connected.

III. Proposed Single-phase Rectifier

A. Topology

After a careful consideration of the aforementioned analysis, it can be found that the current i_C is the key to solve all the problems. First, if i_C is not required to provide dc components, then there is no operational limit caused by loads. Second, if i_C is free from providing the fundamental ripple current, then the fundamental voltage ripples can be completely eliminated. Third, if i_C can be regulated (without introducing any dc or harmonics to the source current), then the two voltage outputs can be controlled independently. Hence, another design freedom should be introduced to enable the regulation of i_C. For this purpose, a current branch is designed by adding the neutral leg proposed in [1] and [16] to the conventional half-bridge rectifier in this paper. The formed topology is composed of a rectification leg and a neutral leg as shown in Fig. 5. The rectification leg inherits the topology and functions from conventional half-bridge rectifiers. The neutral leg is formed by two switches Q_3 and Q_4, an inductor and two split capacitors. The introduction of the neutral leg breaks the constraint on i_C and solves the drawbacks mentioned before.

It is worth noting that the two legs can be controlled independently. The rectification leg can be controlled to regulate the dc-bus voltage, which should be the sum of the two independent voltage outputs, and to draw a sinusoidal current that is in phase with the source voltage. This is quite matured now so the emphasis of this paper is to control the neutral leg so that the two voltages can be independent, with reduced ripples at the fundamental frequency.

B. Model of the Neutral Leg

The midpoint (or average) of the dc bus is

$$V_{\rm ave} = \frac{V_+ - V_-}{2}. \tag{13}$$

According to Kirchhoff's law, there is

$$u_N = L_N\frac{di_L}{dt} + R_N i_L \tag{14}$$

where R_N is the equivalent series resistance of the inductor. Define the currents flowing through the split capacitors are i_{C+} and i_{C-}, respectively. Then

$$i_C = i_{C+} - i_{C-} \tag{15}$$

with

$$i_{C+} = C_+\frac{dV_+}{dt} \tag{16}$$

$$i_{C-} = C_-\frac{dV_-}{dt}. \tag{17}$$

As a result, the dynamic equation of the dc-bus voltage is

$$\begin{aligned}\frac{dV_{\rm DC}}{dt} &= \frac{dV_+}{dt}+\frac{dV_-}{dt}\\ &= \frac{1}{C_+}i_{C+}+\frac{1}{C_-}i_{C-}\\ &= \left(\frac{1}{C_+}+\frac{1}{C_-}\right)i_{C+}-\frac{1}{C_-}i_C\end{aligned} \tag{18}$$

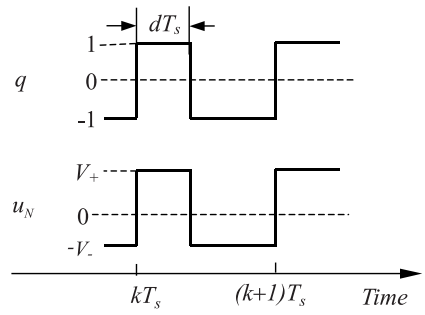

Fig. 6. Signals q and u_N [1].

from which there is

$$i_{C+} = \frac{\frac{dV_{\rm DC}}{dt} + \frac{1}{C_-} i_C}{\frac{1}{C_+} + \frac{1}{C_-}}. \tag{19}$$

Hence, (16) can be rewritten as

$$\begin{aligned} \frac{dV_+}{dt} &= \frac{1}{C_+} \frac{\frac{dV_{\rm DC}}{dt} + \frac{1}{C_-} i_C}{\frac{1}{C_+} + \frac{1}{C_-}} \\ &= \frac{C_-}{C_+ + C_-} \frac{dV_{\rm DC}}{dt} + \frac{1}{C_+ + C_-} i_C. \end{aligned} \tag{20}$$

Since $V_{\rm DC} = V_+ + V_-$, there is

$$\begin{aligned} \frac{dV_-}{dt} &= \frac{dV_{\rm DC}}{dt} - \frac{dV_+}{dt} \\ &= \frac{C_+}{C_+ + C_-} \frac{dV_{\rm DC}}{dt} - \frac{1}{C_+ + C_-} i_C. \end{aligned} \tag{21}$$

Assume that the switching frequency is f_s and the switching period is $T_s = 1/f_s$. Define

$$q = \begin{cases} 1 & \text{when } Q_3 \text{ is on and } Q_4 \text{ is OFF} \\ -1 & \text{when } Q_4 \text{ is on and } Q_3 \text{ is OFF.} \end{cases}$$

Then, the corresponding voltage u_N, together with its given q, can be shown in Fig. 6. Denote the average of q over a switching period by p. Then, $p \in [-1, 1]$ and the duty cycle for Q_3 is

$$d = \frac{1+p}{2}.$$

The average of u_N over a switching period (assuming that V_+ and V_- are constant within a switching period) is approximately

$$u_N = dV_+ - (1-d)V_- = \frac{p}{2} V_{\rm DC} + V_{\rm ave}. \tag{22}$$

Combining (14), (20), (21), and (22), the model of the neutral leg is shown in Fig. 7, where $V_0 = \frac{C_-}{C_+ + C_-} V_{\rm DC}$ plays the role of an external disturbance and p is the control variable.

C. Benefits

1) Removal of the Operational Limit on Loads: The neutral leg provides the path for the source current i_s and the imbalanced current of the dual loads R_+ and R_-. According to Kirchhoff's law, there is

$$i_L = i_s - i_C - I_+ + I_-. \tag{23}$$

If i_C is maintained around 0, then the imbalanced current $I_+ - I_-$ will be provided by the neutral leg but not by the split capacitors any more. The aforementioned operational limit can then be naturally removed. The regulation of the i_C can be done through controlling the control variable p as indicated from the model of the neutral leg in Fig. 7. As a result, the proposed rectifier can work properly no matter what kind of combinations of loads are connected.

2) Reduced Voltage Ripples: From (23), it can be seen that the return source current is provided by the neutral leg, but not by the split capacitors. Hence, the fundamental component of the voltage ripples on the split capacitors can be completely eliminated and the voltage ripples on V_+ and V_- can be reduced.

3) Provision of Independent Voltage Outputs: Assume the references of the two independent dc outputs are V_+^* and V_-^*, respectively, which could be the same or different as long as both of them are higher than the peak value of the source voltage. This is to ensure the boost operation of the rectifier. The dc-bus voltage $V_{\rm DC}$ can then be maintained to be the sum of the two independent outputs by controlling the rectification leg. In other words, the reference for the dc-bus voltage should be set as

$$V_{\rm DC}^* = V_+^* + V_-^*. \tag{24}$$

According to the model of the neutral leg shown in Fig. 7, the dc output V_+ can be regulated via changing control variable p. Then

$$V_+ = V_+^* \tag{25}$$

in the steady state, which also means

$$V_- = V_-^*.$$

Hence, both outputs can be controlled independently.

It is worth mentioning that controlling $i_C = 0$ does not necessarily lead to $V_+ = V_+^*$ because the integrator $\frac{1}{s(C_+ + C_-)}$ (as shown in Fig. 7) may cause the deviation of V_+ from its reference. As a result, when designing the controller for the neutral leg, the regulation of both the current and the voltage should be taken into consideration.

One question that arises naturally is that whether the different voltages V_+ and V_- would cause problems to the input current regulation. As stated previously, the rectification leg and the neutral leg are independently controlled, and as a result, the regulation of the input current only depends on the rectification leg instead of both legs. Indeed, according to (4), the maximum and minimum duty cycles of the two switches in the rectification leg are

$$\begin{aligned} d_{\max} &= \frac{1}{V_{\rm DC}} (V_+ + V_s) \\ d_{\min} &= \frac{1}{V_{\rm DC}} (V_+ - V_s). \end{aligned}$$

Hence, $d_{\min} > 0$ and $d_{\max} < 1$ can be achieved for any combinations of V_+ and V_- that are higher than V_s and the regulation of the input current is not affected by the difference between V_+ and V_-. The only effect of the voltage difference is that the dc offset of the voltage $V_{\rm DC}(1-d)$ across the switch Q_2, which is the same as V_-, is shifted from the midpoint of the dc bus but

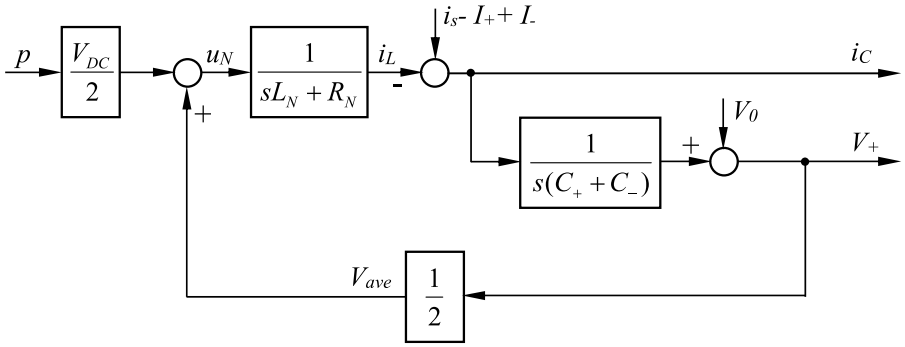

Fig. 7. Model of the neutral leg.

this does not cause any problem. To make it easy to understand, the regulation of the input current is concerned about the dc-bus voltage $V_{\rm DC}$ and it does not matter how this is split between V_+ and V_-, which is achieved by the neutral-leg controller. Because the rectification leg is independently controlled, the input power factor and the THD of the input current can be regulated as usual and are not affected by the difference between V_+ and V_-. Similarly, the effect of any possible dc component in the input voltage is equivalent to the voltage difference between the voltages across the two capacitors, and hence, is limited.

IV. Control Design

A. Control of the Rectification Leg

As analyzed before, one of the main functions for the rectification leg is to regulate the dc-bus voltage. For this purpose, the two dc voltage outputs should be measured for feedback. The sum of them constitute the dc-bus voltage, which contains two parts: a constant component and a ripple component. The constant component should be equal to its reference value $V_+^* + V_-^*$ and the ripple one is normally smoothed by dc-bus capacitors or active energy storage circuits [9], [23], [24]. The constant component should be extracted from the dc-bus voltage for the feedback. Otherwise, the ripple component is introduced into the control loop, which reduces the performance, and hence, should be avoided. Here, the hold filter

$$H(s) = \frac{1 - e^{-Ts/2}}{Ts/2}$$

where T is the fundamental period of the supply, is used to remove the ripple component because the major ripple component is at the second harmonic frequency. A PI controller can then be used to maintain the dc-bus voltage as shown in Fig. 8(a).

In addition to the dc-bus voltage regulation, the rectification leg is also responsible to make sure that the source current i_s is clean and in phase with the source voltage v_s. This reduces the power pollution to the source caused by the rectifier. Considering the power balance at the ac and dc sides, the output of the PI voltage controller is set as the peak amplitude of the reference of i_s. Apart from this amplitude information, the phase information of the source voltage is also needed to form the reference source current. This can be realized in many ways, e.g., with phase-lock loops [25], [26], sinusoid-locked loops [1], or sinusoidal

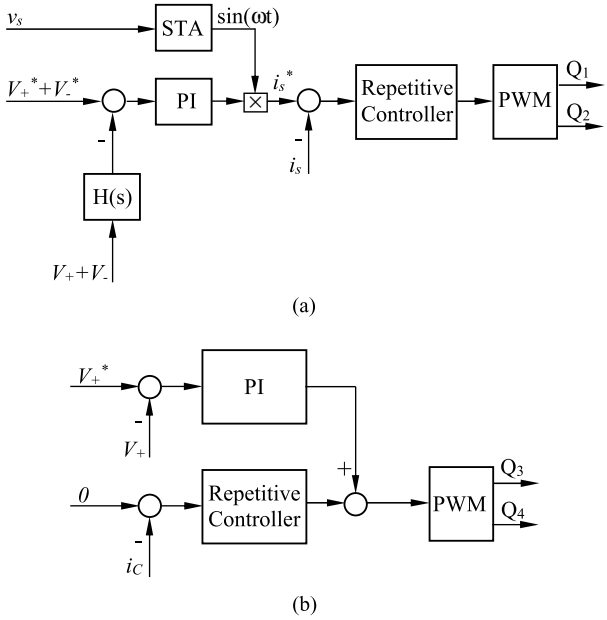

Fig. 8. Controller: (a) for the rectification leg; (b) for the neutral leg.

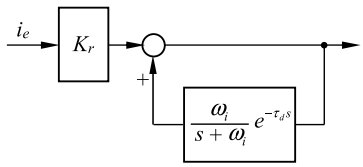

Fig. 9. Repetitive current controller.

tracking algorithms (STA) [27]. Here, the STA proposed in [27] is adopted. With the peak amplitude provided by the PI controller and phase information extracted using the STA, the reference source current i_s^* is then formed. What is left now is to design a current controller so that the current i_s tracks its reference.

Many current controllers, such as hysteresis controllers [28] that have a variable switching frequency and repetitive controllers [29] that have a fixed switching frequency, can be applied to track the current reference i_s^*. Because of the excellent harmonic rejection performance, the repetitive controller shown in Fig. 9 is used, where $i_e = i_s^* - i_s$ is the current tracking error.

The output of the repetitive controller is sent to a PWM generator to generate the PWM signals for the switches Q_1 and Q_2. The repetitive controller consists of a proportional controller K_r and an internal model given by

$$C(s) = \frac{K_r}{1 - \frac{\omega_i}{s+\omega_i} e^{-\tau_d s}}$$

where K_r and τ_d are designed based on the analysis in [1], [29] as

$$\tau_d = \tau - \frac{1}{\omega_i} = 0.0196\,\text{s}$$
$$K_r = \omega_i L_N$$

with L_N chosen close to the neutral inductance and $\omega_i = 2550$, $\tau = 0.02\,\text{s}$.

B. Control of the Neutral Leg

As discussed previously, one of the main tasks of the neutral leg is to maintain the current i_C close to zero. For this purpose, the current i_C should be measured as a feedback to form a current controller. Again, the repetitive controller used in the controller of the rectification leg is adopted here, as shown in Fig. 8(b), to improve the tracking performance. The current i_C is sent to the repetitive controller as an error signal after being subtracted from its reference, which is zero in this case. If $i_C \approx 0$, then $i_L = i_s - I_+ + I_-$ is satisfied. As a result, the function of the neutral leg, providing the return source current and the imbalanced current, is achieved.

However, as can be analyzed from the model of the neutral leg, V_+ could be other values than V_+^* even when $i_c = 0$ because of the existence of the integrator $\frac{1}{s(C_+ + C_-)}$. As a result, another loop is required in order to independently control the two voltage outputs. Because the rectification leg is controlled to maintain the dc-bus voltage at $V_+^* + V_-^*$, it is only necessary to control V_+ to be V_+^*. This can be achieved by using a PI controller. Naturally, $V_- = V_-^*$ can be achieved at the same time. Because this control loop only works at the dc component and the controller that regulates the current i_C only works at non-dc signals, these two controllers can be put into parallel, as done in [1] and [16], by adding the output of the PI voltage controller and the output of the current controller together. The sum is then sent to a PWM block to generate drive signals for Q_3 and Q_4. The resulting controller for the neutral leg is shown in Fig. 8(b).

V. Experimental Validation

The proposed single-phase rectifier controlled by a TMS320F28335 DSP was built up in the lab, with the parameters shown in Table I. In order to demonstrate the independence of the two dc voltage outputs, the three dc loads and split capacitors were chosen to be different on purpose (the capacitors and inductors available in the lab were used so the selection of parameters was not optimized). The coefficients of the PI controller for the dc-bus voltage were chosen by trial-and-error to be $K_P = 0.05$, $K_I = 2$ and the gain of the repetitive controller for the source current i_s was selected as $K_r = 5$. In addition, the parameters of the parallel PI voltage and repetitive current controller were selected as $K_P = 0.1$, $K_I = 3$ and $K_r = 5$, respectively.

TABLE I
Parameters of the Experimental System

Parameters	Values
Supply voltage (RMS)	110 V
Line frequency	50 Hz
L_s	2.2 mH
L_N	2.2 mH
C_+	1120 μF
C_-	560 μF
R	1470 Ω
R_+	470 Ω
R_-	1000 Ω

A. Steady-State Performance

1) With Three Loads $R_+ = 470\ \Omega$, $R_- = 1000\ \Omega$, and $R = 1470\ \Omega$: In this case, both the conventional half-bridge rectifier and the proposed rectifier work but the performances are completely different. The references of the output voltages are set to $V_+^* = 300$ V and $V_-^* = 200$ V. For the conventional half-bridge rectifier, the results are shown in the left column of Fig. 10. Although the dc-bus voltage is around its reference[1], the source current is not sinusoidal. Although $V_+^* > V_-^*$, there was $V_+ < V_-$ in experiments because the two dc voltage outputs are determined by the loads R_+ and R_- and the voltages are not regulated. There are noticeable ripples on both voltage outputs, at the fundamental frequency. For the proposed rectifier, the results are shown in the right column of Fig. 10. The source current is now sinusoidal; the two dc voltage outputs are independently well controlled to be 300 and 200 V (producing a well-controlled dc-bus voltage around 500 V); the ripples on both voltage outputs are much smaller and no fundamental-frequency component is seen.

In order to further compare the ripples of the two cases, the voltage waveforms are zoomed and shown in Fig. 10(c) and (d), respectively. From the view of the frequency, it can be clearly seen that the major component of the ripples is at 50 Hz for the case of the conventional half-bridge rectifier and 100 Hz for the case of the proposed rectifier. This is because all the 50-Hz ripples have been diverted from the capacitors by the neutral leg. From the view of the amplitude, the output voltage ripples of the conventional half-bridge rectifier are 20 and 16 V, respectively. According to (8) and (10), the theoretical ratio of the ripple amplitudes are $\frac{V_- C_-}{V_+ C_+} \approx 1.32$, which is approximately equal to the observed value $\frac{20\,\text{V}}{16\,\text{V}} = 1.25$. As a result, the obtained experimental results are consistent with the theoretical analysis. After starting the neutral leg, the ripple amplitude values are dropped from 20 and 16 V to 3 and 6 V, respectively, as shown in Fig. 10(d). The ratio then becomes $\frac{3\,\text{V}}{6\,\text{V}} = 0.5$, which is the same as the theoretical value $\frac{C_-}{C_+} = 0.5$. Note that in the proposed rectifier, the ripple ratio is no longer dependent on the two

[1]Note that the tolerance of the resistors and the errors in the sensors, etc., have caused some errors in the readings in the figures.

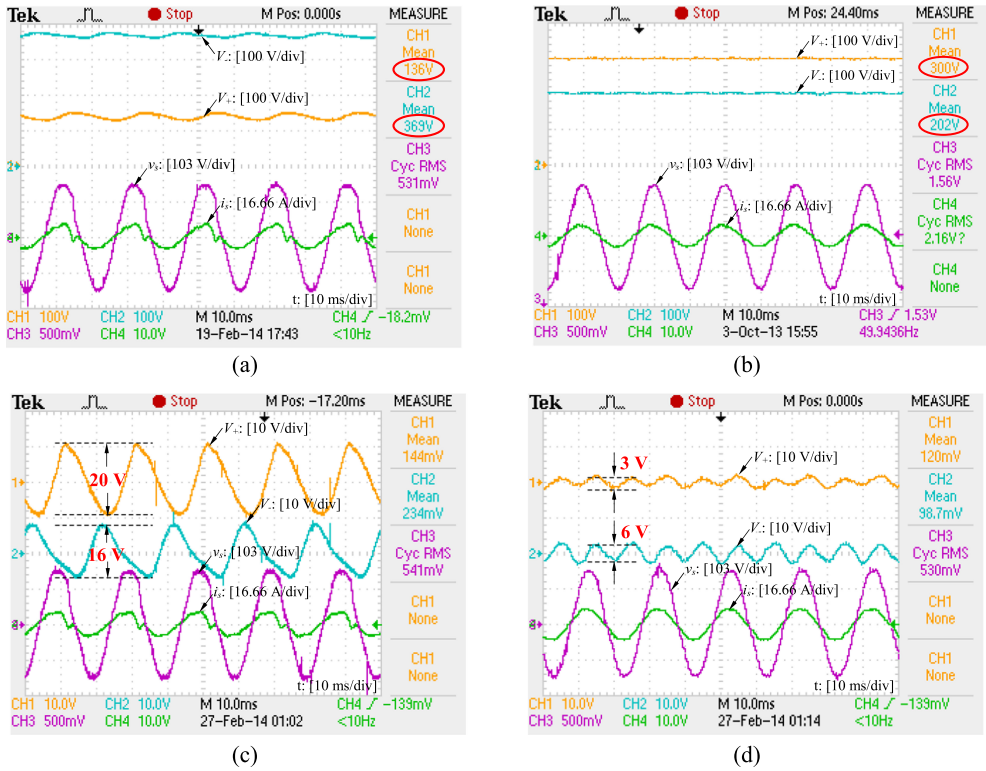

Fig. 10. Steady-state performance with three loads ($V_+^* = 300$ V and $V_-^* = 200$ V): (a) and (c) conventional half-bridge rectifier (without the neutral leg); (b) and (d) proposed rectifier (with the neutral leg).

output voltages but only on the capacitors. In order to clearly show the ripple reduction performance, the voltage V_+ is taken as an example to extract its 50- and 100-Hz ripples from the recorded experimental data with notch filters tuned at 50 and 100 Hz, respectively. For the conventional half-bridge rectifier, the peak–peak values of 50 and 100 Hz ripples are 18 and 2.3 V, respectively. After starting the neutral leg, the peak-peak value of the 50-Hz ripple is significantly reduced to 0.2 V, while the 100-Hz ripple remains more or less the same (because this is not the focus of the paper and no extra effort is taken to deal with the 100-Hz ripples).

In order to further demonstrate the capability of independently regulating the two output voltages, two other experiments were carried out for different voltage references $V_+^* = 250$ V and $V_-^* = 250$ V and $V_+^* = 200$ V and $V_-^* = 300$ V, respectively. The results are shown in Fig. 11. The two output voltages were controlled independently very well.

2) With Only One Load $R_+ = 470\,\Omega$: Another experiment was done to test the proposed rectifier when operated with extremely different loads. Only one of the dual load $R_+ = 470\,\Omega$ was connected. Note that the conventional half-bridge rectifier does not work in this case so no experimental results can be shown. For the proposed rectifier, the results are shown in Fig. 12(a). The output voltages and the source current are regulated very well, without any problem. Moreover, the neutral current was also well maintained around 0 as shown in Fig. 12(b), where the inductor current i_L is also shown. It contains a dc component. According to the analysis in Section III, the inductor current i_L should include a dc bias in this case to offset the current difference between the dual loads R_+ and R_-. Theoretically, the current difference should be

$$\frac{V_+^*}{R_+} - \frac{V_-^*}{R_-} = \frac{300}{470} = 0.6383 \text{ A}$$

which is very close to the bias current 0.64 A observed from Fig. 12(b).

3) Input Power Factor and Input Current THD: For all the aforementioned cases with the same/different loads and/or voltage references, the THD of the input current is about 4.3% and the input power factor is about 0.99, according to the recorded data from experiments. This verifies that the regulation of the input current is not affected by the voltage difference between V_+ and V_-. Note that the experimental system is not optimized for power quality purposes because it is not the focus of this paper. The synchronization unit STA, the hold filter $H(s)$ and the PI controller in the rectification-leg controller shown in Fig. 8(a) could all bring harmonic components into the reference input current. Moreover, the input filter, which is not optimized either, plays an important role in the power quality as well. Hence, the THD of 4.3% for the input current is already very good. It could be improved if the aforementioned factors are taken into consideration.

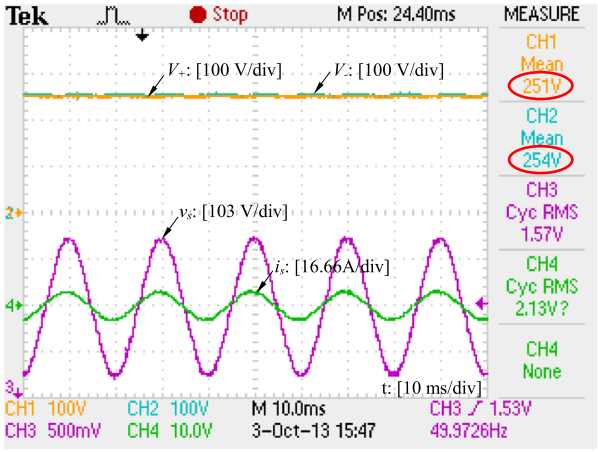

(a)

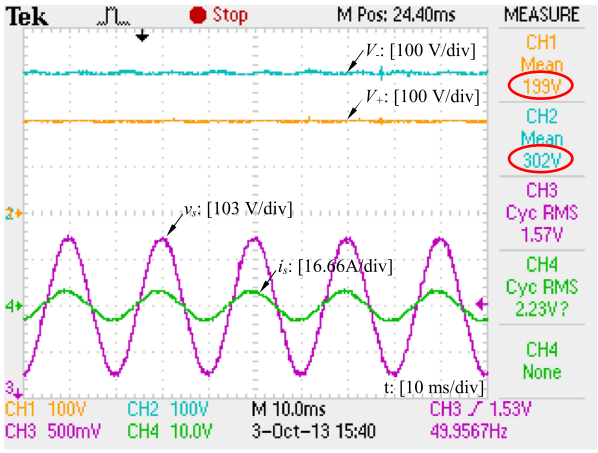

(b)

Fig. 11. Steady-state performance with three loads: (a) $V_+^* = 250$ V and $V_-^* = 250$ V; (b) $V_+^* = 200$ V and $V_-^* = 300$ V.

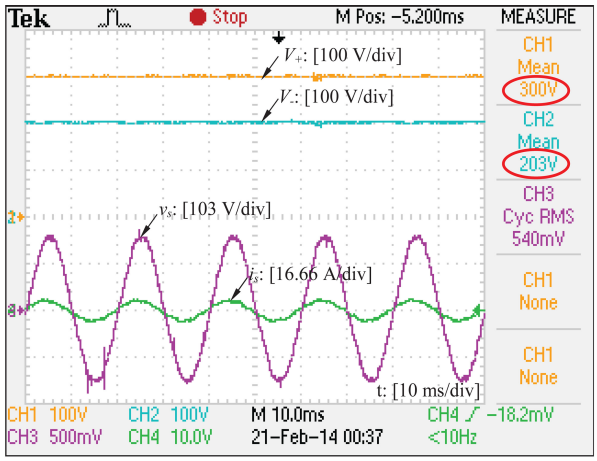

(a)

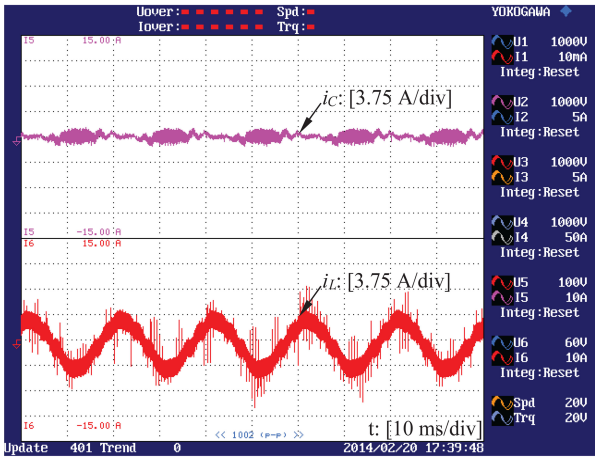

(b)

Fig. 12. Steady-state performance with only one load $R_+ = 470\Omega$ ($V_+^* = 300$ V and $V_-^* = 200$ V): (a) Output voltages, source current, and voltage; (b) Neutral current i_C and auxiliary inductor current i_L.

B. Transient Performance

In order to evaluate the transient performance, three cases are given here as shown in Figs. 13–15. The first two were conducted with the voltage references $V_+^* = 300$ V and $V_-^* = 200$ V. For the third one, the dc voltage references were changed from $V_+^* = 300$ V and $V_-^* = 200$ V to $V_+^* = 200$ V and $V_-^* = 300$ V as a step change.

1) Startup: In the first case, the controllers for the rectification leg and the neutral leg were initially not in function. As a result, the system was operated as a diode bridge rectifier, and therefore, the source current is extremely distorted. Also, the dc outputs were clamped at around 150 V, which is the peak value of the source voltage. Note that the two voltages are slightly different because of the different loads and capacitors. After the controllers were activated, the two voltage outputs quickly increased from 150 V to the reference values of 300 and 200 V, respectively, as shown in Fig. 13. The neutral current i_C was regulated and settled down to nearly 0. This transient response took about 400 ms, which can be reduced if the allowable maximum neutral current is increased (for the current system, it is designed to be 16.66 A).

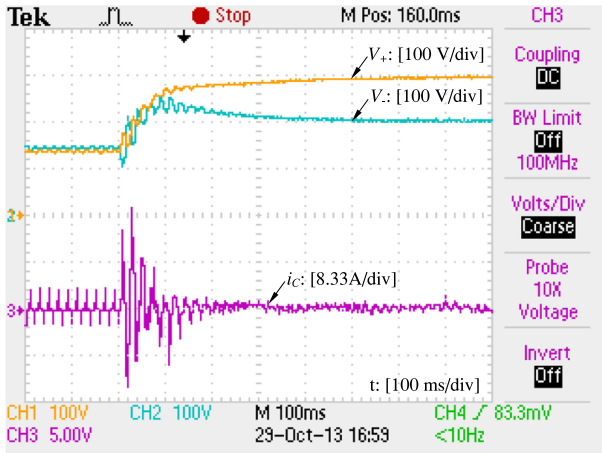

Fig. 13. Start-up: DC outputs V_+ and V_- and neutral current i_C.

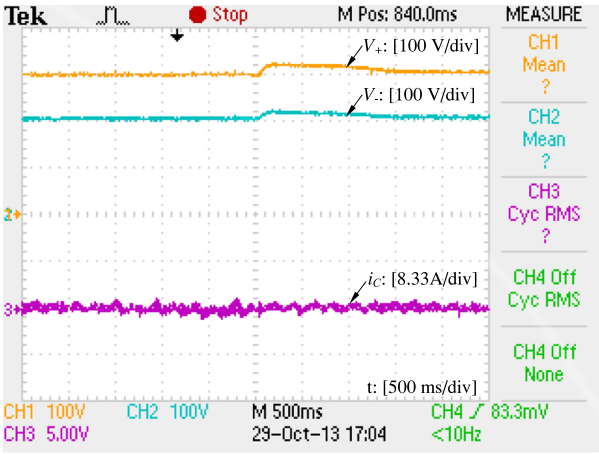

Fig. 14. Load change: DC outputs V_+ and V_- and neutral current i_C.

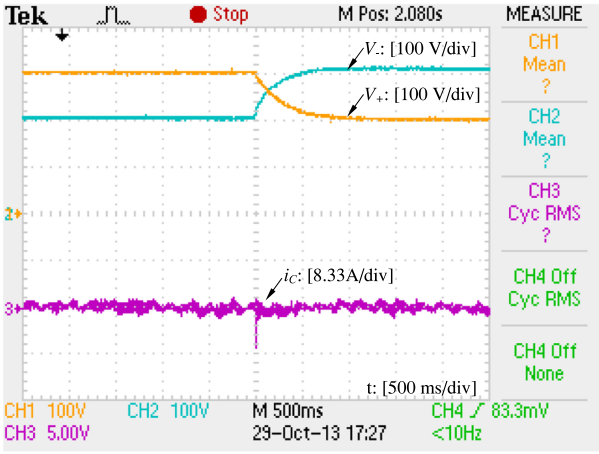

Fig. 15. Transient response when voltage references were changed from $V_+^* = 300$ V and $V_-^* = 200$ V to $V_+^* = 200$ V and $V_-^* = 300$ V: DC outputs V_+ and V_- and neutral current i_C.

2) Load Change: The second case was with a load change and the result is shown in Fig. 14. All the three loads R, R_+, and R_- were initially connected, and then, two of them, R and R_-, were suddenly cutoff from the system. Due to this change, the dc outputs slightly increased, and then, went back to the references without any spikes. The neutral current i_C was always maintained around 0.

3) Change of Voltage References: The last case was the change of the voltage references and the results are shown in Fig. 15. It can be seen that the voltages are smoothly regulated to their new references from previous ones. Again, the neutral current is always around 0 without any noticeable changes. The response time in the last two cases can be shortened by increasing the allowable maximum neutral current.

VI. Comparison with a Typical Solution

It is not easy to identify a suitable topology for comparison because of the functions integrated in the proposed topology. After careful comparison of different topologies, the topology shown in Fig. 16 is adopted for comparison. It is able to provide two isolated dc output voltages in an independent way and adopts the DAB dc/dc converter [30]–[32] cascaded with a front-end PFC converter, which are all very popular topologies. It is possible to connect a third load to the dc bus of the PFC so the system is able to supply three loads at the same time, which is the same as the proposed topology. The DAB converters use only two active switches in order to reduce the losses, and the PFC rectifier only uses one switch so this system is not bidirectional but the proposed topology is bidirectional. In order to make this topology bidirectional, several more active switches need to be added, which will reduce the efficiency. Hence, the system shown in Fig. 16 is a good candidate for comparison apart from the lack of bidirectional capability. The same parameters for the loads, capacitors, active switches, and diodes, etc. are adopted for both systems. It is obvious that the cost of the DAB system is much higher than that of the proposed system for the same capacity, due to the extra high-frequency transformer, the increased number of active switches (five more) and diodes (nine more), and the extra dc-bus capacitor C. If this system is made bidirectional, the cost is going to increase further. Moreover, the DAB system is much more complicated and the reliability is lower because of the increased component count.

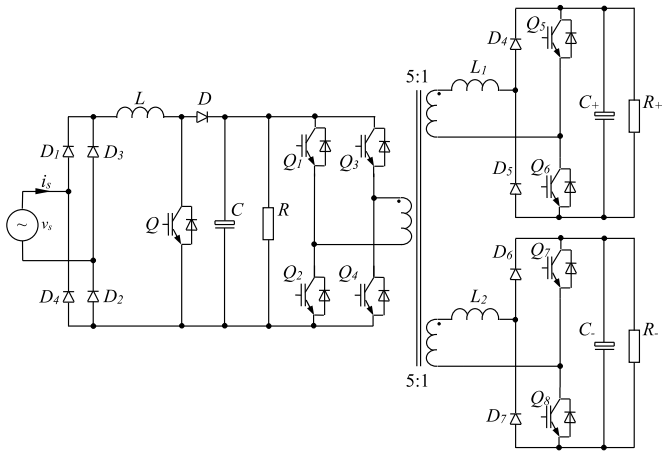

Fig. 16. DAB system used for comparison.

In order to compare their efficiency, both the DAB system and the proposed system were simulated with PLECS, which is able to accurately calculate power losses. The simulations were done with the same parameters for switches and diodes used in both systems. The obtained efficiency curves are shown in Fig. 17. It is clear that the proposed system has higher efficiency compared to the DAB system. This is expected because of the number of switches in the proposed topology is much less than that in the DAB system.

As to the complexity of the control, it is similar for both systems. The control of the rectification leg has a similar level of complexity to the control of the PFC, both with a current regulator, and the control of the neutral leg has a similar level of complexity to the control of the two DAB converters.

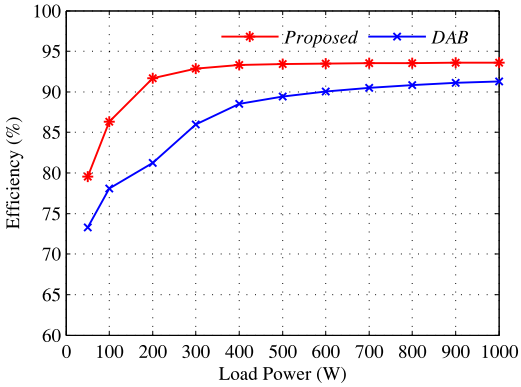

Fig. 17. Efficiency comparison.

Apart from the aforementioned aspects, it is also worth highlighting the important role of the neutral line provided by the proposed topology. For applications like microgrids, a neutral line is necessary if inverters need to supply unbalanced loads and is also needed if both positive and negative voltages are required by loads.

To sum up, as compared to the DAB system, the proposed system has better performance, lower costs and higher efficiency. To be fair, the dc outputs of the DAB system can be higher or lower than the dc-bus voltage but the dc outputs of the proposed system have to be lower than the dc-bus voltage. Hence, the advantage of the proposed topology is obvious.

VII. Conclusion

A single-phase rectifier has been proposed as a unified solution to address the two main drawbacks of conventional half-bridge rectifiers. The proposed rectifier consists of a rectification leg and a neutral leg. The main functions of the rectification leg are to draw a clean current that is in phase with the source voltage and to generate a stable dc-bus voltage. On the other hand, thanks to the neutral leg, the two voltage outputs are independent with each other and are robust against with system parameters. In other words, the proposed rectifier has the capability of coping with different loads and different capacitors. Moreover, the ripples of the output voltages are reduced because the fundamental ripple current is diverted from the capacitors by the neutral leg. Although the capacitors used for experiments are not optimized, it is obvious that the capacitors can be reduced if the level of the voltage ripples is same. Experimental results have demonstrated the capability of the proposed rectifier. Moreover, the comparison with a typical solution that adopts the popular DAB dc/dc converter cascaded with a front-end PFC converter has shown that the proposed topology offers better performance, lower cost, higher reliability, and higher efficiency. A possible improvement is to add shoot-through function to the topology to improve the reliability, which will be reported in the future.

Acknowledgment

The authors would like to thank Yokogawa Measurement Technologies, Ltd. for the donation of a high-precision wide-bandwidth power meter WT1600.

References

[1] Q.-C. Zhong and T. Hornik, *Control of Power Inverters in Renewable Energy and Smart Grid Integration*. New York, NY, USA: Wiley-IEEE Press, 2013.

[2] R. Machado, S. Buso, and J. Pomilio, "A line-interactive single-phase to three-phase converter system," *IEEE Trans. Power Electron.*, vol. 21, no. 6, pp. 1628–1636, Nov. 2006.

[3] D. Dong, I. Cvetkovic, D. Boroyevich, W. Zhang, R. Wang, and P. Mattavelli, "Grid-interface bidirectional converter for residential DC distribution systems—Part one: High-density two-stage topology," *IEEE Trans. Power Electron.*, vol. 28, no. 4, pp. 1655–1666, Apr. 2013.

[4] D. Dong, F. Luo, X. Zhang, D. Boroyevich, and P. Mattavelli, "Grid-interface bidirectional converter for residential DC distribution systems—Part 2: AC and DC interface design with passive components minimization," *IEEE Trans. Power Electron.*, vol. 28, no. 4, pp. 1667–1679, Apr. 2013.

[5] K. Yao, X. Ruan, X. Mao, and Z. Ye, "Reducing storage capacitor of a DCM Boost PFC converter," *IEEE Trans. Power Electron.*, vol. 27, no. 1, pp. 151–160, Jan. 2012.

[6] K. Yao, X. Ruan, X. MAo, and Z. Ye, "Variable-duty-cycle control to achieve high input power factor for DCM boost PFC converter," *IEEE Trans. Ind. Electron.*, vol. 58, no. 5, pp. 1856–1865, May 2011.

[7] Y.-K. Lo, T.-H. Song, and H.-J. Chiu, "Analysis and elimination of voltage imbalance between the split capacitors in half-bridge boost rectifiers," *IEEE Trans. Ind. Electron.*, vol. 49, no. 5, pp. 1175–1177, Oct. 2002.

[8] Y.-K. Lo, C.-T. Ho, and J.-M. Wang, "Elimination of the output voltage imbalance in a half-bridge boost rectifier," *IEEE Trans. Power Electron.*, vol. 22, no. 4, pp. 1352–1360, Jul. 2007.

[9] R. Wang, F. Wang, D. Boroyevich, R. Burgos, R. Lai, P. Ning, and K. Rajashekara, "A high power density single-phase PWM rectifier with active ripple energy storage," *IEEE Trans. Power Electron.*, vol. 26, no. 5, pp. 1430–1443, May 2011.

[10] X. Zhang and C. Gong, "Dual-buck half-bridge voltage balancer," *IEEE Trans. Ind. Electron.*, vol. 60, no. 8, pp. 3157–3164, Aug. 2013.

[11] R. Srinivasan and R. Oruganti, "A unity power factor converter using half-bridge boost topology," *IEEE Trans. Power Electron.*, vol. 13, no. 3, pp. 487–500, May 1998.

[12] C. Liu and J.-S. Lai, "Low frequency current ripple reduction technique with active control in a fuel cell power system with inverter load," *IEEE Trans. Power Electron.*, vol. 22, no. 4, pp. 1429–1436, Jul. 2007.

[13] R.-J. Wai and C.-Y. Lin, "Active low-frequency ripple control for clean-energy power-conditioning mechanism," *IEEE Trans. Ind. Electron.*, vol. 57, no. 11, pp. 3780–3792, Nov. 2010.

[14] J.-I. Itoh and F. Hayashi, "Ripple current reduction of a fuel cell for a single-phase isolated converter using a DC active filter with a center tap," *IEEE Trans. Power Electron.*, vol. 25, no. 3, pp. 550 –556, Mar. 2010.

[15] J. C. Salmon, "Circuit topologies for single-phase voltage-doubler boost rectifiers," *IEEE Trans. Power Electron.*, vol. 8, no. 4, pp. 521–529, Oct. 1993.

[16] T. Hornik and Q.-C. Zhong, "Parallel PI voltage–H^{∞} current controller for the neutral point of a three-phase inverter," *IEEE Trans. Ind. Electron.*, vol. 60, no. 4, pp. 1335–1343, Apr. 2013.

[17] Q.-C. Zhong and T. Hornik, "Cascaded current-voltage control to improve the power quality for a grid-connected inverter with a local load," *IEEE Trans. Ind. Electron.*, vol. 60, no. 4, pp. 1344–1355, Apr. 2013.

[18] T. S. Win, Y. Baba, E. Hiraki, T. Tanaka, and M. Okamoto, "A half-bridge inverter based active power quality compensator using a constant DC capacitor voltage control for electrified railways," in *Proc. 7th Int. Power Electron. Motion Control Conf.*, 2012, vol. 1, pp. 314–320.

[19] C. Zhang, D. Jiang, H. Zheng, and L. Ye, "A bi-directional buck/boost voltage balancer for DC distribution system," in *Proc. 4th Int. Conf. Digital Manuf. Autom.*, 2013, pp. 9–13.

[20] B. Wang, X. Ruan, K. Yao, and M. Xu, "A method of reducing the peak-to-average ratio of LED current for electrolytic capacitor-less AC–DC drivers," *IEEE Trans. Power Electron.*, vol. 25, no. 3, pp. 592–601, Mar. 2010.

[21] P. Krein, R. Balog, and M. Mirjafari, "Minimum energy and capacitance requirements for single-phase inverters and rectifiers using a ripple port," *IEEE Trans. Power Electron.*, vol. 27, no. 11, pp. 4690–4698, Nov. 2012.

[22] T. Hornik and Q.-C. Zhong, "H^{∞} repetitive voltage control of grid-connected inverters with frequency adaptive mechanism," *IET Proc. Power Electron.*, vol. 3, no. 6, pp. 925–935, Nov. 2010.

[23] X. Zhang, X. Ruan, H. Kim, and C. K. Tse, "Adaptive active capacitor converter for improving stability of cascaded DC power supply system," *IEEE Trans. Power Electron.*, vol. 28, no. 4, pp. 1807–1816, Apr. 2013.

[24] S. Wang, X. Ruan, K. Yao, S.-C. Tan, Y. Yang, and Z. Ye, "A flicker-free electrolytic capacitor-less ac–dc LED driver," *IEEE Trans. Power Electron.*, vol. 27, no. 11, pp. 4540–4548, Nov. 2012.
[25] C. da Silva, R. Pereira, L. da Silva, G. Lambert-Torres, B. Bose, and S. Ahn, "A digital PLL scheme for three-phase system using modified synchronous reference frame," *IEEE Trans. Ind. Electron.*, vol. 57, no. 11, pp. 3814–3821, Nov. 2010.
[26] P. Rodriguez, J. Pou, J. Bergas, J. Candela, R. Burgos, and D. Boroyevich, "Decoupled double synchronous reference frame PLL for power converters control," *IEEE Trans. Power Electron.*, vol. 22, no. 2, pp. 584–592, Mar. 2007.
[27] A. K. Ziarani and A. Konrad, "A method of extraction of nonstationary sinusoids," *Signal Process.*, vol. 84, no. 8, pp. 1323–1346, Apr. 2004.
[28] A. Tilli and A. Tonielli, "Sequential design of hysteresis current controller for three-phase inverter," *IEEE Trans. Ind. Electron.*, vol. 45, no. 5, pp. 771–781, Oct. 1998.
[29] T. Hornik and Q.-C. Zhong, "A current control strategy for voltage-source inverters in microgrids based on H^{∞} and repetitive control," *IEEE Trans. Power Electron.*, vol. 26, no. 3, pp. 943–952, Mar. 2011.
[30] H. Qin and J. Kimball, "Closed-loop control of DC–DC dual-active-bridge converters driving single-phase inverters," *IEEE Trans. Power Electron.*, vol. 29, no. 2, pp. 1006–1017, Feb. 2014.
[31] H. Qin and J.W. Kimball, "Generalized average modeling of dual active bridge DC–DC converter," *IEEE Trans. Power Electron.*, vol. 27, no. 4, pp. 2078–2084, Apr. 2012.
[32] J. Kan, S. Xie, Y. Tang, and Y. Wu, "Voltage-fed dual active bridge bidirectional DC/DC converter with an immittance network," *IEEE Trans. Power Electron.*, vol. 29, no. 7, pp. 3582–3590, Jul. 2014.

Wen-Long Ming received the B.Eng. and M.Eng. degrees in automation from Shandong University, Jinan, China, in 2007 and 2010, respectively. He is currently working toward the Ph.D. degree in the Department of Automatic Control and Systems Engineering, University of Sheffield, Sheffield, U.K.

He was with Center for Power Electronics Systems, Virginia Tech, Blacksburg, VA, USA, in 2012 as an Academic Visiting Scholar. His research interests include reliability of dc-bus capacitors, technology to reduce passive components, traction power systems, transformerless PV inverters, and neutral line provision in power electronic systems.

Qing-Chang Zhong (M'04–SM'04) received the Ph.D. degree in control and engineering from Shanghai Jiao Tong University, Shanghai, China, in 2000, and the Ph.D. degree in control theory and power engineering from Imperial College London, London, U.K., in 2004.

He is the Chair Professor in control and systems engineering at the Department of Automatic Control and Systems Engineering, University of Sheffield, Sheffield, U.K., and a Specialist recognized by the State Grid Corporation of China. He is a Distinguished Lecturer of the IEEE Power Electronics Society and the UK Representative to the European Control Association. He coauthored three research monographs: Control of Power Inverters in Renewable Energy and Smart Grid Integration (New York, NY, USA: Wiley-IEEE Press, 2013), Robust Control of Time-Delay Systems (New York, NY, USA: Springer-Verlag, 2006), Control of Integral Processes with Dead Time (New York, NY, USA: Springer-Verlag, 2010), and a fourth, Completely Autonomous Power Systems (CAPS): Next Generation Smart Grids, is scheduled for publication by Wiley-IEEE Press in 2015. He proposed the architecture for the next-generation smart grids based on the synchronization mechanism of synchronous machines to achieve autonomous operation for power systems. His research interests include power electronics, advanced control theory and the integration of both, together with applications in renewable energy, smart grid integration, electric drives and electric vehicles, aircraft power systems, high-speed trains, etc.

Dr. Zhong received the Best Doctoral Thesis Prize from Imperial College London. He serves on the University Technology Partnership Board of Rolls-Royce Plc and the Scientific Advisory Board of FREEDM Systems Center at North Carolina State University. He is a Fellow of the Institution of Engineering and Technology, the Vice Chair of the IFAC TC of Power and Energy Systems and was a Senior Research Fellow of the Royal Academy of Engineering/Leverhulme Trust, U.K. (2009–2010). He serves as an Associate Editor for the IEEE TRANSACTIONS ON AUTOMATIC CONTROL, the IEEE TRANSACTIONS ON POWER ELECTRONICS, the IEEE TRANSACTIONS ON INDUSTRIAL ELECTRONICS, the IEEE TRANSACTIONS ON CONTROL SYSTEMS TECHNOLOGY, IEEE ACCESS, the IEEE JOURNAL OF EMERGING AND SELECTED TOPICS IN POWER ELECTRONICS, the *European Journal of Control*, and the Conference Editorial Board of the IEEE Control Systems Society.